Genes to Cells

Efficient TALEN construction and evaluation methods for human cell and animal applications

Tetsushi Sakuma[1], Sayaka Hosoi[1], Knut Woltjen[2], Ken-ichi Suzuki[1], Keiko Kashiwagi[3], Housei Wada[4], Hiroshi Ochiai[5], Tatsuo Miyamoto[5], Narudo Kawai[6], Yasunori Sasakura[7], Shinya Matsuura[5], Yasushi Okada[8], Atsuo Kawahara[8], Shigeo Hayashi[4,9] and Takashi Yamamoto[1]*

[1]*Department of Mathematical and Life Sciences, Graduate School of Science, Hiroshima University, 1-3-1 Kagamiyama, Higashi-Hiroshima, Hiroshima 739-8526, Japan*
[2]*Center for iPS Cell Research and Application (CiRA), Kyoto University, 53 Shogoin-Kawahara-cho, Sakyo-ku, Kyoto 606-8507, Japan*
[3]*Institute for Amphibian Biology, Graduate School of Science, Hiroshima University, 1-3-1 Kagamiyama, Higashi-Hiroshima, Hiroshima 739-8526, Japan*
[4]*Laboratory for Morphogenetic Signaling, RIKEN Center for Developmental Biology, 2-2-3 Minatojima-minamimachi, Chuo-ku, Kobe, Hyogo 650-0047, Japan*
[5]*Department of Genetics and Cell Biology, Research Institute for Radiation Biology and Medicine, Hiroshima University, 1-2-3 Kasumi, Minami-ku, Hiroshima 734-8553, Japan*
[6]*Department of Biology, Research and Education Center for Natural Sciences, Keio University, 4-1-1 Hiyoshi, Kohoku-ku, Yokohama 223-8521, Japan*
[7]*Shimoda Marine Research Center, University of Tsukuba, 5-10-1 Shimoda, Shizuoka 415-0025, Japan*
[8]*Quantitative Biology Center, RIKEN, 6-2-3 Furuedai, Suita, Osaka 565-0874, Japan*
[9]*Department of Biology, Graduate School of Science, Kobe University, 1-1 Rokkodai-cho, Nada-ku, Kobe, Hyogo 657-8051, Japan*

Transcription activator–like effector nucleases (TALENs) have recently arisen as effective tools for targeted genome engineering. Here, we report streamlined methods for the construction and evaluation of TALENs based on the 'Golden Gate TALEN and TAL Effector Kit' (Addgene). We diminished array vector requirements and increased assembly rates using six-module concatemerization. We altered the architecture of the native TALEN protein to increase nuclease activity and replaced the final destination vector with a mammalian expression/*in vitro* transcription vector bearing both CMV and T7 promoters. Using our methods, the whole process, from initiating construction to completing evaluation directly in mammalian cells, requires only 1 week. Furthermore, TALENs constructed in this manner may be directly applied to transfection of cultured cells or mRNA synthesis for use in animals and embryos. In this article, we show genomic modification of HEK293T cells, human induced pluripotent stem cells, *Drosophila melanogaster*, *Danio rerio* and *Xenopus laevis*, using custom-made TALENs constructed and evaluated with our protocol. Our methods are more time efficient compared with conventional yeast-based evaluation methods and provide a more accessible and effective protocol for the application of TALENs in various model organisms.

Introduction

Genome editing with artificial nucleases is hailed as a next-generation technology, enhancing gene targeting in previously nonpermissive model organisms (McMahon *et al.* 2012). Artificial nuclease pairs comprise specific, juxtaposed DNA-binding domains and nonspecific nuclease domains, which dimerize to induce DNA double-strand breaks (DSBs) at targeted loci, triggering endogenous repair pathways and stimulating homologous recombination (de Souza

Communicated by: Masayuki Miura
**Correspondence*: tybig@hiroshima-u.ac.jp

DOI: 10.1111/gtc.12037

2012). So far, zinc-fingers (ZFs) and transcription activator-like effectors (TALEs) have been developed to provide custom-engineered DNA-binding proteins. Fused to the FokI nuclease domain, both zinc-finger nucleases (ZFNs) and TALE nucleases (TALENs) have been shown to be effective for genome editing in cultured cells and various organisms (Urnov *et al.* 2010; Carroll 2011; Mussolino & Cathomen 2012).

Between the two nuclease technologies, there are clear advantages and disadvantages. ZFNs generally comprised three to six ZF domains that recognize 9–18-bp DNA, whose protein size is much more compact than that of TALEs. However, tandem repeats of ZF domains are known to interfere with each other, making effective construction of *de novo* ZF arrays difficult (Cathomen & Joung 2008). TALEs, however, show no context dependency and thus may be designed relatively easily (Bogdanove & Voytas 2011). The DNA recognition code of TALEs comprises only two amino acid variations, known as a repeat-variable di-residue (RVD), in a highly conserved 34 amino acid repeat unit that binds one nucleotide (Boch *et al.* 2009). In accordance with this advantage of TALENs, many methods to construct designer TALEs have been reported (Cermak *et al.* 2011; Li *et al.* 2011, 2012; Morbitzer *et al.* 2011; Sander *et al.* 2011; Weber *et al.* 2011; Zhang *et al.* 2011; Briggs *et al.* 2012; Reyon *et al.* 2012). One of the most popular open-source TALEN construction kits, the 'Golden Gate TALEN and TAL Effector Kit', is available from Addgene (Cambridge, MA). This kit contains 72 vectors, including TALE DNA-binding module plasmids, vector plasmids for the intermediary arrays and the final destination vectors containing the *Xanthomonas oryzae* pv. Oryzae-derived PthXo1-based TALE scaffold is well characterized, along with AvrBs3 from *X. campestris* pv. vesicatoria (Christian *et al.* 2010). Serial assembly of modules is based on a cycling type IIs restriction endonuclease reaction, reportedly taking only 5 days for TALEN construction (Cermak *et al.* 2011). Yet, the rate of success in independent laboratories is variable.

Importantly, many aspects of this new TALEN technology remain uncertain; in particular, how to optimize fusion of the DNA-binding and nuclease domains. Recent studies have shown that various truncations of the N- and C-terminal regions of the native TALE proteins affect DSB-forming activity (Miller *et al.* 2011; Mussolino *et al.* 2011; Sun *et al.* 2012).

To apply TALENs as a standardized technology in various model organisms, evaluation methods and criteria for constructed TALENs and derivatives stand as additional bottlenecks. Presently, *in vitro* cleavage assays and yeast-based assay systems are mainly used for the evaluation of custom-made TALENs (Cermak *et al.* 2011; Li *et al.* 2011, 2012; Mahfouz *et al.* 2011). These systems are robust but time-consuming, and it is unclear whether the activities *in vitro* or in yeast parallel that of higher eukaryotes including animal embryos and cultured cells. Cel-I or T7 endonuclease I cleavage assays directly screen DSB-forming activity by detecting imperfect nonhomologous end-joining repair induced by TALENs (Hockemeyer *et al.* 2011; Reyon *et al.* 2012; Sanjana *et al.* 2012). Such cleavage assays are suitable for direct evaluation of TALEN activity against their intended endogenous genes, but, unlike *in vitro* assays, are cell line or animal dependent and not necessarily applicable as universal TALEN validation assays. Furthermore, application of TALENs in essential model animals has gradually been realized by various independent groups using different TALEN architectures (Huang *et al.* 2011; Sander *et al.* 2011; Tesson *et al.* 2011; Wood *et al.* 2011; Cade *et al.* 2012; Liu *et al.* 2012; Moore *et al.* 2012), yet still no systematic methods exist which cover the construction and evaluation of TALENs that can be commonly used for all such cells and animals.

Here, we report unified methods for the construction and evaluation of TALENs, and we furthermore show the effectiveness of our TALENs. We modified vector constructs and protocols based on the 'Golden Gate TALEN and TAL Effector Kit', not only clarifying assembly but also TALEN evaluation and application. We show that re-engineering the TALEN architecture enhances activity in assays and practical applications. Furthermore, we validated our tools and TALEN construction methods by successful endogenous gene modification of cultured cells and multiple animal species. Our method ensures a convenient and reliable system of custom TALEN development for use in various cells and animal applications.

Results

Adaptations permitting rapid construction of custom TALENs

We first modified the intermediary array vectors of the 'Golden Gate TALEN and TAL Effector Kit'

to realize more robust first-step assembly. On a trial basis, we found that less than six-module ligation showed reproducible results in various independent laboratories. On average, success rate of ten-module assembly was approximately 10%, meanwhile success rate of six-module assembly was almost 100% in our groups. Additionally, like the original kit, six modules permit the construction of TALENs with up to thirty-one repeats without increasing the number of cloning steps (Fig. 1A). To incorporate our six-module ligation system to the Voytas kit, we have only to replace the pFUS_A, A30A and A30B capture vectors with our pFUS_A1A, A2A, A2B, A3A, A3B, A4A and A4B capture vectors. Note that pFUS_A3C and A4D are identical to pFUS_A2B, and pFUS_A4C is identical to pFUS_A3B. In using these specialized 6-module capture vectors, we decrease the number of RVD module vectors by 40% (from 40 to 24), minimizing efforts for RVD plasmid library preparation and the complexity of the first Golden Gate reaction. As TALEN technology is in a highly dynamic phase of development, this adaptation ensures that incorporation of new variant RVD vectors, such as NH and NK, recently shown to provide more context-relevant 'G' nucleotide recognition (Streubel *et al.* 2012), will require reduced effort. By simply incorporating our vectors into the original kit, we diminish the efficiency barrier of the first Golden Gate cloning step.

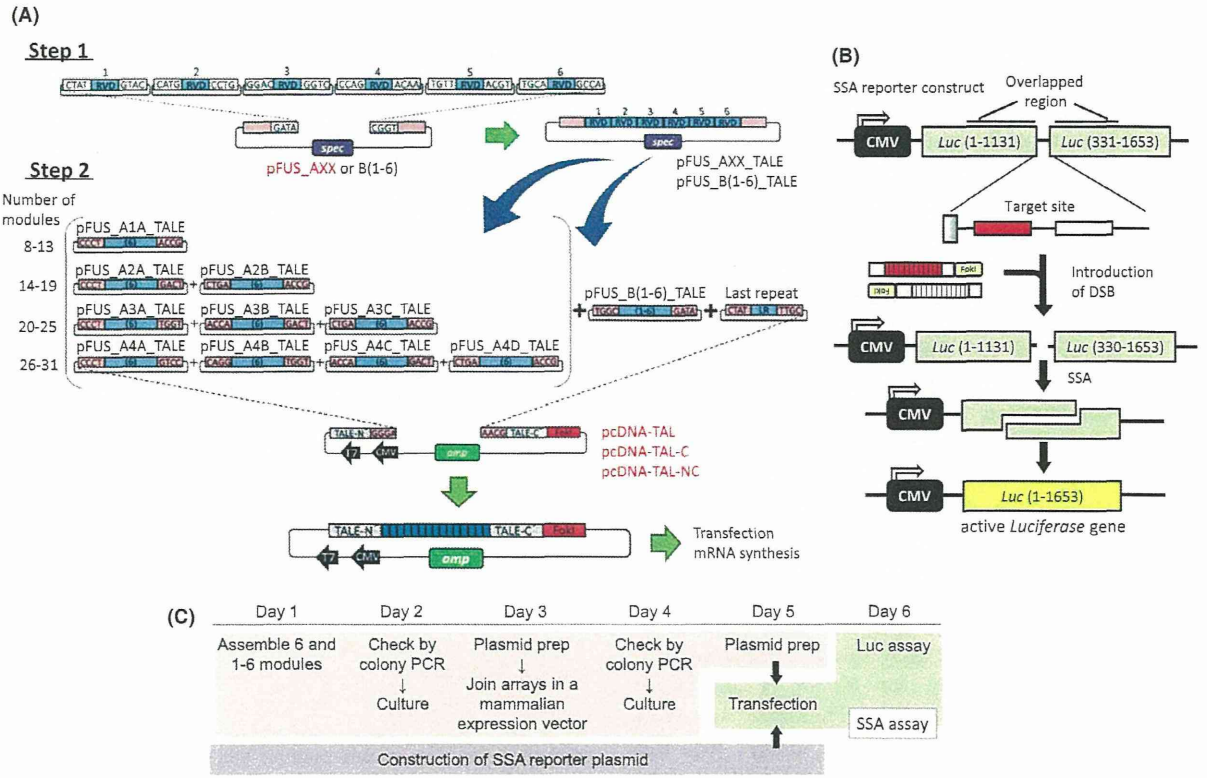

Figure 1 Simplified method for the rapid construction and evaluation of custom TALENs. (A) Schematic overview of the six-module assembly method. Six or less than six modules are ligated into array plasmids in a first step. Subsequently, constructed arrays are joined into a mammalian expression vector in a second step. Bases in white and pink boxes represent overhangs left by BsaI and Esp3I, respectively. The vectors typed in red are modified vectors from the original kit. Spec, spectinomycin; Amp, ampicillin; CMV, cytomegalovirus promoter. (B) Scheme of the SSA assay. HEK293T cells were transfected with three types of plasmids, comprising TALEN-expressing plasmids, a reporter plasmid and a reference plasmid for dual-luciferase assay. The reporter plasmid encodes two split inactive parts of the luciferase gene with overlapping repeated sequences. Following a DSB caused by the TALENs, a functional luciferase gene is generated by an SSA reaction. (C) Timeline of TALEN construction and evaluation. It takes only 5 days for the construction and the evaluation of the activity completes in day six.

TALEN activity in HEK293T-based SSA assay parallels genome modification frequency

Next, we converted the evaluation system to a mammalian cell-based SSA assay (Fig. 1B), which has been previously characterized for the evaluation of ZFN activity in cultured cells and several animal embryo applications (Ochiai *et al.* 2010, 2012; Ansai *et al.* 2012; Kawai *et al.* 2012; Song *et al.* 2012; Watanabe *et al.* 2012). To conveniently transition constructed TALENs to a human cell–based assay, we replaced the capture vector of the second Golden Gate assembly step with a mammalian expression vector bearing cytomegalovirus (CMV) and T7 promoters (Fig. 1A). As the result, assembled TALEN plasmids can be directly used in the SSA assay, transfection into target cells or mRNA synthesis for embryo injection without additional cloning. These improvements allow us to construct, evaluate and apply custom TALENs easily and quickly (Fig. 1C).

To validate the mammalian cell–based SSA assay (Fig. 2A), we constructed *HPRT1*_B TALENs similar to those originally described in the Cermak paper (Cermak *et al.* 2011). Compared with cells transfected with TALENs and a reporter vector bearing unrelated target sequences, cells transfected with TALENs and the associated SSA reporter showed marked activation in a dose-dependent manner (Fig. 2A). Additional previously reported TALENs *HPRT1*_A, *CFTR*_A, *CFTR*_B, *GFP* and *eGFP*_A (Cermak *et al.* 2011) were similarly constructed using our 6-module construction system. As *eGFP*-A TALENs showed low activity in the previous article (Cermak *et al.* 2011), we designed and constructed another TALEN pair for the *eGFP* gene in addition to them (*eGFP*_B). Our SSA assay showed that constructed TALENs had a variety of activities (Fig. 2B). Interestingly, despite the full accordance of amino acid sequences, the previously reported yeast-based assay and our HEK293T-based assay showed disparate TALEN activities, especially for *CFTR*_A and *GFP* (Cermak *et al.* 2011) (Fig. 2B). Therefore, we used the Cel-I assay (Guschin *et al.* 2010) for the *HPRT1*_A, *HPRT1*_B, *CFTR*_A and *CFTR*_B TALENs (Fig. 2C) as readout for direct genome modification. By using Cel-I nuclease, amount of mutated DNAs can be easily measured. After the TALEN introduction, PCR amplification around target sequence, followed by denaturation and reannealing, is carried out so that they can generate heteroduplexes when TALENs induce mutations. As Cel-I nuclease digests DNAs with base-mismatches, we can

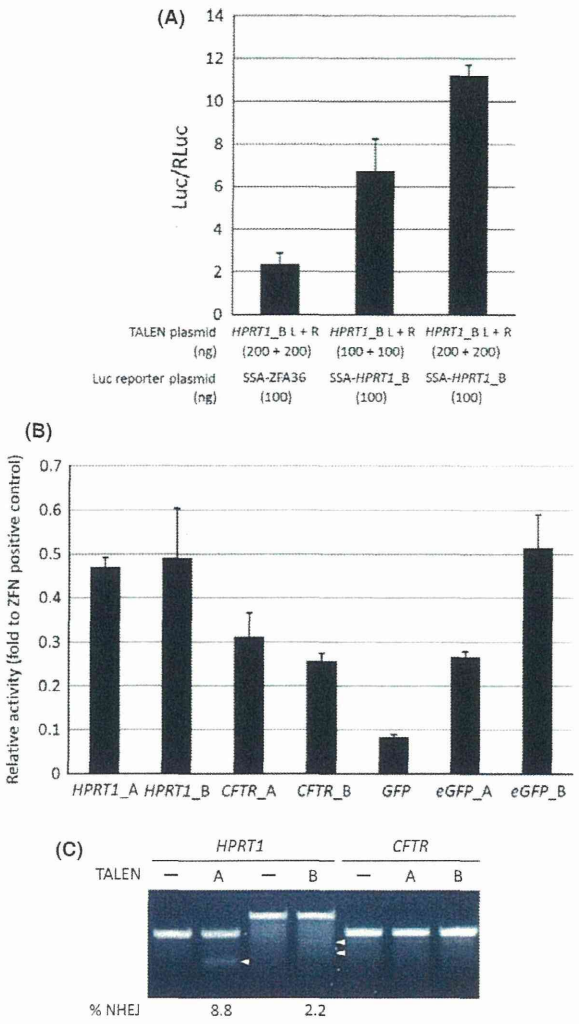

Figure 2 Functional evaluation of engineered TALENs by SSA and Cel-I assay. (A) Evaluation of SSA activity of a TALEN pair targeted to human gene, *HPRT1*. Data are expressed as means ± SEM ($n = 3$). (B) Comparison of the activity of several custom TALENs by SSA assay. Relative activity is defined as the ratio of measured activity to the activity score of pSTL-ZFA36. Data are expressed as means ± SEM ($n = 3$). (C) Cel-I assay using custom TALENs for human genes. Arrowheads indicate the expected positions of the digested products. % NHEJ (nonhomologous end joining) was estimated using ImageJ software as previously described (Hansen *et al.* 2012).

analyze approximate mutation rate by simple electrophoresis of Cel-I-digested product. As a result, cleaved products appeared in the *HPRT1*_A or *HPRT1*_B TALEN-treated genomes, but no cleaved products were observed in the *CFTR*_A or *CFTR*_B

TALEN-treated genomes, showing some correlation with our SSA assay data (Fig. 2B,C). In contrast, the previous yeast-based assay showed that *CFTR*_A TALEN had higher activity than *HPRT1*_A (Cermak *et al.* 2011), which is strikingly different from our Cel-I data. These results suggest that our HEK293T cell-based SSA assay system represents a relatively accurate activity score compared with the yeast-based assay, at least in human cells.

N- and C-terminal deletions of PthXo1 TALE scaffold increase TALEN activity

Based on the previous report that describes deletion scaffolds of AvrBs-based TALENs with high activity and low toxicity (Mussolino *et al.* 2011), we similarly designed N- and C-terminal truncated PthXo1-based TALENs without disrupting the native N-terminal nuclear localization signal (NLS; Fig. 3A). In the previous article, TALENs with a +153 N-terminal domain and a +47 C-terminal domain, named NC scaffold, showed the highest cleavage activity when separated by 12 to 15 bp spacer lengths (Mussolino *et al.* 2011). Therefore, we constructed truncation variants of *HPRT1*_B TALENs, named *HPRT1*_B TALEN-C and *HPRT1*_B TALEN-NC, and evaluated them both by SSA and Cel-I assays (Fig. 3A–C). TALEN-C retains a full N-terminal domain and +47 C-terminal domain, whereas TALEN-NC has a +153 N-terminal domain and +47 C-terminal domain (Fig. 3A). RVD arrays may be assembled directly in these truncation variants by the usual Golden Gate cloning method with pcDNA-TAL-C or pcDNA-TAL-NC capture vectors instead of pcDNA-TAL. SSA assay results using reporter constructs containing 7, 11 and 15 spacer sequences showed that our truncation variants had higher activity than the original TALENs when the spacer length was 11 or 15 bp (2- to 2.5-fold), consistent with the previous report using analogous AvrBs-based truncations (Mussolino *et al.* 2011) (Fig. 3C). Furthermore, we observed the efficiency of genome modification by these TALEN variants using the Cel-I nuclease assay (Fig. 3B). The *HPRT1*_B TALEN-NC pair showed higher activity compared with the original, thus confirming the usefulness of our deletion scaffolds.

Truncated PthXo1-based TALEN architecture achieves homozygous gene disruption in hiPSC

To assess the functionality of our TALEN-NC architecture, we made use of an HPRT disruption assay in

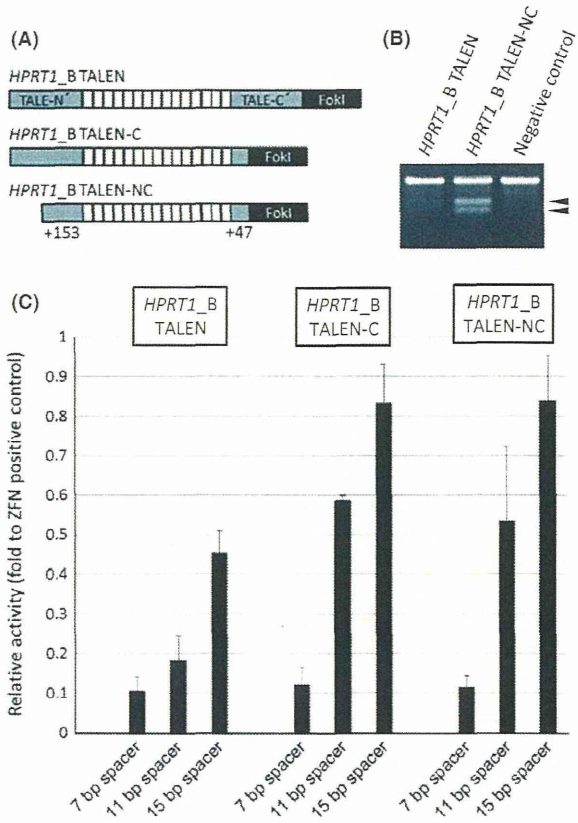

Figure 3 N- and C-terminal deletions of the TALE scaffold enhanced the activity of the *HPRT1*_B TALENs. (A) Schematic of TALENs harboring original scaffold and truncated scaffold. (B) Cel-I assay. Arrowheads indicate the expected positions of the digested products. (C) Relative TALEN activity in relation to spacer length measured by SSA assay. Relative activity is defined as the ratio of measured activity to the activity score of pSTL-ZFA36. Data are expressed as means ± SEM (n = 3).

human induced pluripotent stem cells (hiPSCs). The *HPRT1* gene is X-linked and a component of the purine salvage pathway, permitting drug counter-selection (Caskey & Kruh 1979). Whereas HPRT1$^{+/+}$ cells are 6-thioguanine sensitive (6-TG^{S}) and resistant to hypoxanthine, aminopterin and thymidine (HAT^{R}), HPRT1$^{-/-}$ cells are 6-thioguanine resistant (6-TG^{R}) and hypoxanthine, aminopterin and thymidine sensitive (HAT^{S}). The hiPSC line 201B7 is derived from female fibroblasts (Takahashi *et al.* 2007) and has been shown to have two active X-chromosomes (Tomoda *et al.* 2012); thus, TALEN-induced resistance to 6-TG would require disruption of both copies of the HPRT gene. Spontaneous inactivation

of HPRT is extremely rare (Thomas & Capecchi 1987).

We electroporated the *HPRT1*_B TALEN or TALEN-NC expression vectors into female 201B7 hiPSCs. After 6-TG selection, cells electroporated with the original TALEN architecture were unable to form colonies, suggesting a homozygous disruption rate below the sensitivity level of this assay. Conversely, cells electroporated with the TALEN-NC pair consistently formed colonies (Fig. 4A,B). Under these conditions, electroporation of only the left or right TALEN gave rise only to rare false positives devoid of mutation in the PCR-screened target region (clone 201L2, Fig. 4C). All clones transfected with the *HPRT1*_B TALEN-NC pair were HAT^S, indicating true functional knockout events (Fig. 4C). Furthermore, sequence analysis of the TALEN target site showed that TALEN-induced 6-TG resistance is the result of compound heterozygous InDels spanning the spacer region (Fig. S1 in Supporting Information). These results confirm the utility of the engineered TALEN-NC scaffold in hiPSCs.

TALEN-mediated disruption of exogenous eGFP transgenes in various animals

To elucidate the utility of our TALEN architecture for animal applications, we examined whether our uniquely constructed *eGFP*_B TALENs could disrupt integrated *eGFP* transgenes in flies, frogs and zebrafish. First, we tested *eGFP*_B TALEN-mediated gene knockout in the fly, *Drosophila melanogaster*. We used the protein trap line, P{PTT-GA}Jupiter[G00147] (Morin *et al.* 2001), bearing an actively expressing eGFP insertion at the *Jupiter* locus and a second eGFP insertion at a silent locus for TALEN injection. Among 79 embryos injected, 35 grew up to fertile adults (44%). Among 35 vials of fertile cross, seven $eGFP^-$ progeny, with at least one allele disrupted, were obtained (20%, Table 1). Fourteen eGFP-negative progenies were balanced, and their eGFP coding regions sequenced (Fig. 5). At least one of the two eGFP insertions was disrupted, and double mutations were found in three cases. Most of eGFP mutations caused frame shifts and reduced viability of homozygous flies. Because the original protein trap line is homozygous viable, our eGFP knockout lines are thought to be new *Jupiter* mutants. Further phenotypic characterization is underway.

Based on the success of invertebrate gene knockouts, we applied the same *eGFP_B* TALEN set to the vertebrates, *Danio rerio* (zebrafish) and *Xenopus laevis* (frog). In the case of zebrafish, we crossed *Tg(flk1:mRFP)* lines and *Tg(fli1a:eGFP)* lines, which express mRFP and eGFP in vascular endothelial cells, respectively. Subsequently, TALENs were injected at one- to four-cell stages of the double transgenic embryos. Small populations of endothelial cells judged by mRFP expression were completely suppressed in eGFP expression, suggesting the mosaic disruption of the eGFP transgene in the F_0 progenitors (Fig. 6A–C). Consistent with this observation, *eGFP* gene modification was confirmed by Cel-I assay (Fig. 6D).

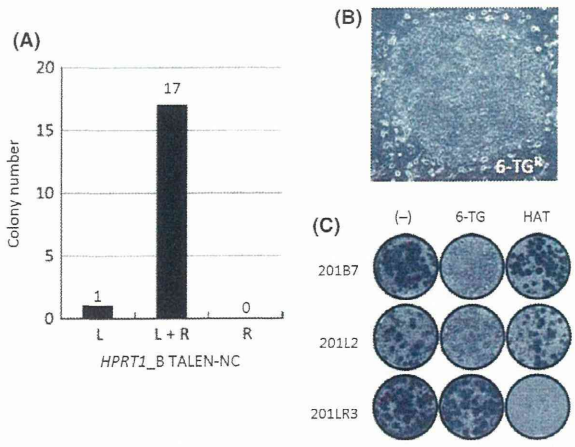

Figure 4 HPRT1 homozygous knockout in female human iPSCs. (A) Number of 6-TG^R colonies. Data are expressed as means. (B) Normal morphology of a 6-TG^R $HPRT^{-/-}$ hiPSC colony. (C) Crystal violet staining of cultures after 4 days of 6-TG or HAT selection. Clones 201B7, 201L2 and 201LR3 display representative growth properties of parental, nontargeted and targeted cells, respectively.

Table 1 Summary of TALEN-induced mutagenesis after microinjection of mRNAs into *Drosophila melanogaster*

F_1		F_2	
eGFP+ only	eGFP− progeny	eGFP+	eGFP−
28	7	95	4
		125	10
		132	2
		91	11
		50	22
		52	7
		90	6

Deletions

```
WT ttCTTCAAGGACGACGGCAACTacaagacccgcgccgAGGTGAAGTTCGAGGGCGac
   ttCTTCAAGGACGACGGCAACTacaagacc---gccgAGGTGAAGTTCGAGGGCGac
   ttCTTCAAGGACGACGGCAACTacaag-----cgccgAGGTGAAGTTCGAGGGCGac
   ttCTTCAAGGACCACGGCAACTacaag-----------GTGAAGTTCGAGGGCGac*
   ttCTTCAAGGACGACGGCAACTac-------gcgccgAGGTGAAGTTCGAGGGCGac
   ttCTTCAAGGACGACGGCAACTaca-gacccgcgccgAGGTGAAGTTCGAGGGCGac
   ttCTTCAAGGACGACGGCAACTacaag-----------GTGAAGTTCGAGGGCGac*
   ttCTTCAAGGACGACGGC---------------gccgAGGTGAAGTTCGAGGGCGac
   ttCTTCAAGGACGACGGCA-----------cgcgccgAGGTGAAGTTCGAGGGCGac
```

Complex types

```
WT ttCTTCAAGGACGACGGCAACTacaagacc---------cgcgccgAGGTGAAGTTCGAGGGCGac
   ttCTTCAAGGACGACGGCAACTacaagGTGA----------cgccgAGGTGAAGTTCGAGGGCGac
   ttCTTCAAGGACGACGGCAACTaGGACGACG---------gcgccgAGGTGAAGTTCGAGGGCGac
   ttCTTCAAGGACGACGGCAACTacaagT-----------cgcgccgAGGTGAAGTTCGAGGGCGac
   ttCTTCAAGGACGACGGCAACTacaagTTCAAGTTCAA----------GTGAAGTTCGAGGGCGac
   ttCTTCAAGGACGACGGCAACTacGCCGTCTACTACTACTAcgccgAGGTGAAGTTCGAGGGCGac
   ttCTTCAAGGACGACGGCAACTacaaCTACTA-------cgcgccgAGGTGAAGTTCGAGGGCGac
```

Figure 5 Sequences observed in eGFP knockout *D. melanogaster* lines. The wild-type sequence of *eGFP* is shown at the top with the TALEN-targeting sequences (capital letters). Deletions are indicated by dashes and insertions by capital letters with an underline. Asterisks indicate the same mutation types from independent lines.

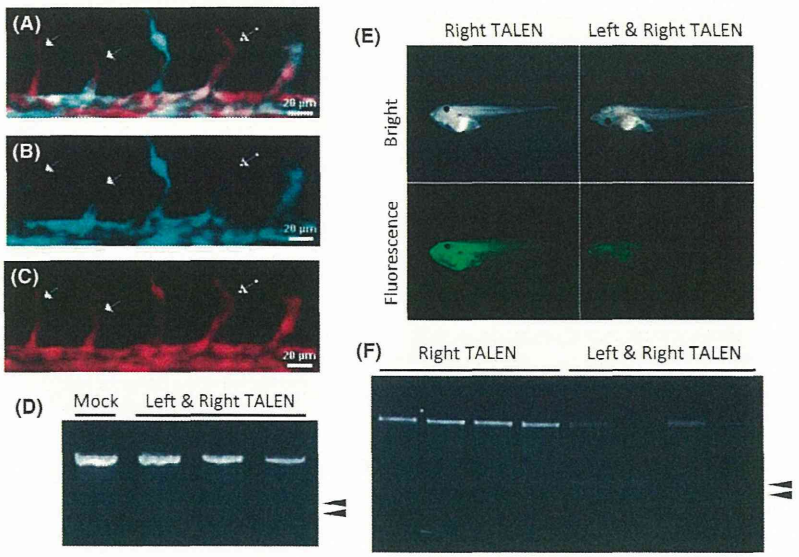

Figure 6 Transcription activator–like effector nuclease-mediated eGFP disruption in vertebrates. (A–C) Fluorescence microscopy images of *eGFP*_B TALEN-injected zebrafish embryos. *eGFP*_B TALEN mRNAs (100 pg each) were injected at 1–4 cell stage zebrafish embryos obtained by reciprocal crossing of *Tg(fli1a:eGFP)* and *Tg(flk1:mRFP)*. A merged image is shown in panel a, eGFP fluorescence is shown in panel b, and mRFP fluorescence is shown in panel (C). The eGFP expression in a small population of endothelial cells indicated by arrows was specifically suppressed, presumably due to the disruption of *eGFP* locus by the TALEN. Similar mosaic eGFP expression was observed in eight independent embryos. (D) Cel-1 assay of Mock or TALEN-injected zebrafish embryos. Arrowheads indicate Cel-1-digested fragments. (E) Bright field and fluorescence microscopy images of *eGFP*_B TALEN-injected frog embryos. (F) Cel-1 assay of TALEN-injected frog embryos. Arrowheads indicate Cel-1 digested fragments. Right: A tadpole injected 600 pg right *eGFP*_B TALEN mRNA. Left and Right: A tadpole injected each 300 pg of left and right *eGFP*_B TALENs mRNA.

Meanwhile, much more dramatic TALEN effects were observed in frogs. We used *in vitro* fertilized eggs of ubiquitously expressing eGFP *Tg(CMV:eGFP)* lines for injection. Surprisingly, maternally transmitted eGFP expression of the TALEN-injected F_0 progenies nearly vanished in most embryos (Fig. 6E). We

obtained the similar results in *Tg(CMV:eGFP)* transgene disruption for paternal transmission (Fig. S2 in Supporting Information). Furthermore, the Cel-I assay showed that mutation rates of *eGFP* genes were extremely high compared with the results obtained using zebrafish (Fig. 6D,F). High-frequency *eGFP* gene mutation was also confirmed by DNA sequence analysis (Fig. S3 in Supporting Information).

Discussion

The 'Golden Gate TALEN and TAL Effector Kit' from the Voytas laboratory implements a two-step assembly method to make custom TAL effector–based constructs, including TALEs and TALENs in yeast expression vectors (Cermak *et al.* 2011). This sophisticated assembly system is particularly appealing compared with other open-source TALEN construction kits available (www.addgene.org/TALEN). The 'TALE Toolbox kit', supplied from the Zhang laboratory, is based on a PCR-mediated rapid assembly system to make the constructs with a standard of 18.5 TALE repeats. Limitations with this kit are the potential for PCR-generated errors and a lower flexibility in repeat lengths, which in turn confounds sequence confirmation. 'TAL Effector Engineering Reagents', supplied from the Joung laboratory, are based on the REAL (Restriction Enzyme And Ligation) assembly method. This method can precisely assemble TALE repeats, but completing the construction is time-consuming. Recently, the Joung laboratory developed an automated assembly method, FLASH (fast ligation-based automatable solid-phase high-throughput) (Reyon *et al.* 2012). It is currently the fastest assembly method, but requires significant start-up costs sophisticated equipment and a huge amount of effort to maintain. The investment of time and resources required is suitable only for laboratories intending large-scale construction of TALENs.

Taking overall comparison into account, the Golden Gate kit is thought to be the best choice to make custom-made TALENs rapidly and precisely in a casual laboratory scale. However, there still remain some issues in the kit to be resolved, especially for animal applications. The first-step assembly method of the original kit requires ten-module ligation using Golden Gate cloning, which the robustness of the reaction is typically not high enough to be widely applied. In addition, the original evaluation system is yeast-based, which takes too much time and possesses lower reliability in the measured activity for the animal cells and embryos.

In this study, we have successfully developed and used simplified methods for TALEN construction and evaluation and showed the availability of our TALEN architecture. Based on the Golden Gate kit, we have minimized the required components for construction, while increasing efficacy. Using our protocol, the whole process, from construction to evaluation in mammalian cells, can be completed within 1 week. With this system, we succeeded in high-efficiency genome modification in various cells including HEK293T cells and hiPSCs. In addition, we showed the disruption of exogenous eGFP transgenes in flies, zebrafish and frogs using TALENs. We expect that our system will reduce barriers faced by entry-level TALEN application in cells and animals. Toward this end, the vectors described herein and additionally constructed CMV early enhancer/chicken beta actin (CAG) promoter-driven destination vector will be deposited in Addgene for public access, contributing globally to genome editing research.

Experimental procedures

Backbone vector construction

pFUS_A1A, A2A, A2B, A3A, A3B, A3C, A4A, A4B, A4C, A4D plasmids were constructed by inverse PCR using the primers listed in Table S1 in Supporting Information. For the construction of the final capture vector pcDNA-TAL, a SacI/BglII fragment from pTAL4 (Cermak *et al.* 2011) was inserted into pcDNA3.1 (Invitrogen, Carlsbad, CA, USA). Deletion constructs of pcDNA-TAL (pcDNA-TAL-C or pcDNA-TAL-NC) were constructed by inverse PCR using the primers listed in Table S1 in Supporting Information.

Construction of TALEN expression plasmids

The protocol for TALEN assembly follows the original report (Cermak *et al.* 2011) with some key modifications. The new 6-module backbone vectors for intermediary arrays are depicted in Fig. 1A. Repeat assembly was conducted using a Golden Gate reaction, transformed to XL1-Blue competent cells and screened precisely assembled clones by colony PCR using the pCR8_F1 and pCR8_R1 primers (Cermak *et al.* 2011). Constructed array plasmids and the appropriate last repeat are captured during a second Golden Gate reaction in the mammalian expression vectors, pcDNA-TAL, pcDNA-TAL-C or pcDNA-TAL-NC, described above. Final assembly, transformation and colony PCR screening for the second Golden Gate reaction followed the previous report (Cermak *et al.* 2011).

For consistency in analysis, TALEN plasmids used in this article were mainly designed to recapitulate those of the previous report (Cermak *et al.* 2011) with the exception of

*eGFP*_B TALENs. Target sequences of *eGFP*_B TALENs are as follows: left 5′-CTTCAAGGACGACGGCAACT-3′ and right 5′-CGCCCTCGAACTTCACCT-3′.

Construction of SSA reporter plasmids

Transcription activator–like effector nuclease plasmids constructed using this modified protocol may be immediately evaluated using a single-strand annealing (SSA) assay. The pGL4-SSA reporter vector, containing inactive fragments of the luciferase gene that bear 700-bp regions of homologous overlap and are driven by a cytomegalovirus (CMV) immediate-early enhancer/promoter, was generated as described previously (Ochiai *et al.* 2010). For the addition of TALEN target sequences, sense and antisense oligonucleotides (Table S2 in Supporting Information) were annealed and inserted into BsaI sites between the bisected luciferase elements of pGL4-SSA.

pGL4-SSA-*HPRT1*_B-7 and pGL4-SSA-*HPRT1*_B-15 were constructed using restriction enzymes and T4 DNA polymerase (Takara Bio, Otsu, Japan). Plasmid pGL4-SSA-*HPRT1*_B-11 was digested with SacI or XhoI, and protruding ends of these DNA fragments were resected or filled in using T4 DNA polymerase. Polished fragments were then self-ligated to obtain pGL4-SSA-*HPRT1*_B-7 and pGL4-SSA-*HPRT1*_B-15, respectively.

SSA assay using HEK293T cells

The SSA assay was carried out as previously described (Ochiai *et al.* 2010) with slight modifications. HEK293T cells were grown in DMEM supplemented with 10% FCS. Fifty thousand cells were cotransfected with 200 ng of each of the TALEN expression plasmids, 100 ng of the pGL4-SSA reporter plasmid and 20 ng of the pRL-CMV reference vector (Promega, Madison, WI, USA) using Lipofectamine LTX (Invitrogen) in a 96-well plate. After 24 h, dual-luciferase assays were conducted using the Dual-Glo luciferase assay system (Promega) in a TriStar LB 941 plate reader (Berthold Technologies, Bad Wildbad, Germany) following the manufacturer's instructions. For the ZFN-positive control, a ZFN expression vector, pSTL-ZFA36, was constructed as previously described (Ochiai *et al.* 2010) and co-transfected with reporter plasmids as described herein.

Transfection and Cel-I assay

Transfection for the Cel-I assay was carried out as follows: the day before transfection, 150 000 HEK293T cells were plated to 35-mm dishes. The day of transfection, 1.5 μg of TALEN plasmids was transfected using Lipofectamine LTX (Invitrogen) according to manufacturer's instructions. The day after transfection, cells were moved to 60-mm dishes. At 72 h post-transfection, cells were collected and their genomic DNA isolated with the DNeasy Blood & Tissue Kit (Qiagen, Hilden, Germany). Genomic PCR was carried out with primers listed in Table S3 in Supporting Information. Amplified products were purified (PCR Purification Kit, Qiagen), and 400 ng of purified DNA was used for the SURVEYOR Mutation Detection Kit Cel-I assay (Transgenomic, Omaha, NE, USA) according to manufacturer's instructions. Products were analyzed by electrophoresis in 3% agarose gels and ethidium bromide staining.

6-Thioguanine (6-TG) screening of HPRT$^{-/-}$ human induced pluripotent stem cells (hiPSCs)

The female human iPS cell line 201B7 was derived from fibroblasts using retroviral reprogramming vectors (Takahashi *et al.* 2007). Maintenance of 201B7 and TALEN-targeted derivatives was carried out on SNL feeder cells in ReproCELL media as described.

*HPRT1*_B TALENs were transferred by standard cloning into a human iPS cell transient expression vector driven by the CAG promoter (Niwa *et al.* 1991). TALEN-mediated gene disruption was carried out using transient transfection by electroporation with the Neon system (Invitrogen). 1×10^6 viable 201B7 cells prepared by feeder depletion and single-cell dissociation with Accutase (Stemcell Technologies, Vancouver, Canada) were electroporated with 5 μg of each TALEN pair (1400 V, 20 ms, 1 pulse, 100 μL Neon tip). Cells were plated at a density of 15 000 cells/cm^2 in hiPSC media containing Rho-Kinase inhibitor (Y-27632; Wako, Osaka, Japan). Two days after electroporation, the media were changed to 15 μM 6-TG (A-4660; Sigma, St. Louis, MO, USA)-containing media, and reduced to 5 μM between days 8 and 10. Compact colonies were counted and picked for expansion and genotyping in the absence of drug. Counter-selection with 1x HAT (H0262; Sigma) was carried out during standard cell passage.

Genomic DNA was isolated from 6-TG^R iPS cell clones using the DNeasy Blood and Tissue Kit (Qiagen). Genomic PCR was carried out with forward and reverse *HPRT1*_B primers (Table S3 in Supporting Information). Products were analyzed by gel electrophoresis, TA-cloned into pGEM-T (Promega), and the resulting plasmids sequenced by standard dye-terminator chemistry and analyzed on an ABI 3130x. Sequences alignments to determine insertions and deletions were carried out with Sequencer (Genecodes, Ann Arbor, MI, USA).

eGFP-transgenic fly and zebrafish strains

For gene disruption in *Drosophila*, a strain containing a homozygous third chromosome protein trap insertion in the *Jupiter* gene (encoding a microtubule-binding protein) P{PTT-GA}Jupiter [G00147] (Morin *et al.* 2001), and P{Ubi-tagRFP.CAAX}TK1 (Kondo and Hayashi, submitted) inserted into the attP site at the cytogenetic location 68A4 (Groth *et al.* 2004), was used. During the course of this study, an additional nonfluorescent insertion of P{PTT-GA} was discovered in this strain.

To establish *Tg(flk1:mRFP)* fish, both a Tol2 transposon plasmid containing a 7-kb flk1 promoter element driving

mRFP and Tol2 transposase mRNA were co-injected into the blastomere of one-cell stage embryos. After these embryos were raised to adulthood *Tg(flk1:mRFP)*^{ko09}, which stably expresses mRFP in vascular endothelial cells was isolated. Another endothelial reporter transgenic fish *Tg(fli1a:EGFP)*^{y1} was also used (Lawson & Weinstein 2002).

mRNA synthesis, embryo microinjection and Cel-I assay

Constructed and evaluated *eGFP*_B TALEN plasmids were used for mRNA synthesis directly from the pcDNA-TAL vector. TALEN plasmids were linearized by restriction enzyme digestion and were used as templates in mRNA synthesis using the mMessage mMachine T7 Ultra Kit (Ambion, Austin, TX, USA) following the manufacturer's instructions. Microinjection into animal embryos was carried out as follows:

Fly: Dechorionated *Drosophila* embryos were injected with 250 μg/mL each of synthetic eGFP_B TALEN mRNA at their posterior ends. All of eclosed adults expressed normal levels of eGFP and tagRFP, and among 35 fertile crosses, seven yielded eGFP-, tagRFP+ progenies that were analyzed by PCR amplification and DNA sequencing.

Zebrafish: *eGFP*_B TALEN mRNA pairs (100 pg each) were injected at 1- to 4-cell stage zebrafish embryos obtained by reciprocal crossing of *Tg(fli1a:EGFP)*^{y1} and *Tg(flk1:mRFP)*^{ko09}. The embryos, anesthetized with tricaine, were observed with PlanApo20x/0.75 objective (Nikon, Tokyo, Japan) at 33 h postfertilization. Optically sectioned images of intersegmental veins were obtained with a laser scanning confocal microscope A1-VAAS (Nikon). Maximum projection image of the volume data is presented. Genomic DNA was recovered from each embryo for Cel-I assay after microscopic examination. eGFP was amplified from the genome with KOD-FX-Neo polymerase (TOYOBO, Osaka, Japan) using the primers described in Table S3 in Supporting Information. The amplified fragment was used for Cel-I assays, and digested products were analyzed by electrophoresis in 1% Synergel (Diversified Biotech, Boston, MA, USA) and ethidium bromide staining.

Frog: *In vitro* fertilized eggs were obtained by mating *CMV:eGFP*-transgenic lines with wild type of *X. laevis* adults. Six hundred picograms of eGFP TALEN mRNA was injected into one-cell stage embryos. Injected embryos were reared to the swimming tadpole stage and then were observed through a fluorescence stereomicroscope. Cel-I assay was carried out as described above.

Acknowledgements

We thank Sumihare Noji and Keishi Osakabe for discussions. We also thank Akihiko Kashiwagi and Nobuaki Furuno for assistance in frog experiments. We appreciate Kikumi Horiguchi for assistance in TALEN construction and Hidehiko Kawai for construction of CAG promoter-driven destination vector. The authors wish to express their thanks to Dr Daniel Voytas for supplying the Golden Gate TALEN and TAL Effector Kit (Addgene, TALEN kit #1000000016). The authors also thank the Cryogenic Center of Hiroshima University for supplying liquid nitrogen. This study was supported by a Grant-in-Aid for Scientific Research on Innovative Areas (No. 2020006) to T.Y. and a Grant-in-Aid for JSPS Fellows (No. 12J06938) to T.S.

References

Ansai, S., Ochiai, H., Kanie, Y., Kamei, Y., Gou, Y., Kitano, T., Yamamoto, T. & Kinoshita, M. (2012) Targeted disruption of exogenous EGFP gene in medaka using zinc-finger nucleases. *Dev. Growth Differ.* **54**, 546–556.

Boch, J., Scholze, H., Schornack, S., Landgraf, A., Hahn, S., Kay, S., Lahaye, T., Nickstadt, A. & Bonas, U. (2009) Breaking the code of DNA binding specificity of TAL-type III effectors. *Science* **326**, 1509–1512.

Bogdanove, A.J. & Voytas, D.F. (2011) TAL effectors: customizable proteins for DNA targeting. *Science* **333**, 1843–1846.

Briggs, A.W., Rios, X., Chari, R., Yang, L., Zhang, F., Mali, P. & Church, G.M. (2012) Iterative capped assembly: rapid and scalable synthesis of repeat-module DNA such as TAL effectors from individual monomers. *Nucleic Acids Res.* **40**, e117.

Cade, L., Reyon, D., Hwang, W.Y., Tsai, S.Q., Patel, S., Khayter, C., Joung, J.K., Sander, J.D., Peterson, R.T. & Yeh, J.R. (2012) Highly efficient generation of heritable zebrafish gene mutations using homo- and heterodimeric TALENs. *Nucleic Acids Res.* **40**, 8001–8010.

Carroll, D. (2011) Genome engineering with zinc-finger nucleases. *Genetics* **188**, 773–782.

Caskey, C.T. & Kruh, G.D. (1979) The HPRT locus. *Cell* **16**, 1–9.

Cathomen, T. & Joung, J.K. (2008) Zinc-finger nucleases: the next generation emerges. *Mol. Ther.* **16**, 1200–1207.

Cermak, T., Doyle, E.L., Christian, M., Wang, L., Zhang, Y., Schmidt, C., Baller, J.A., Somia, N.V., Bogdanove, A.J. & Voytas, D.F. (2011) Efficient design and assembly of custom TALEN and other TAL effector-based constructs for DNA targeting. *Nucleic Acids Res.* **39**, e82.

Christian, M., Cermak, T., Doyle, E.L., Schmidt, C., Zhang, F., Hummel, A., Bogdanove, A.J. & Voytas, D.F. (2010) Targeting DNA double-strand breaks with TAL effector nucleases. *Genetics* **186**, 757–761.

Groth, A.C., Fish, M., Nusse, R. & Calos, M.P. (2004) Construction of transgenic Drosophila by using the site-specific integrase from phage phiC31. *Genetics* **166**, 1775–1782.

Guschin, D.Y., Waite, A.J., Katibah, G.E., Miller, J.C., Holmes, M.C. & Rebar, E.J. (2010) A rapid and general assay for monitoring endogenous gene modification. *Methods Mol. Biol.* **649**, 247–256.

Hansen, K., Coussens, M.J., Sago, J., Subramanian, S., Gjoka, M. & Briner, D. (2012) Genome editing with CompoZr custom zinc finger nucleases (ZFNs). *J. Vis. Exp.*, e3304.

Hockemeyer, D., Wang, H., Kiani, S., *et al.* (2011) Genetic engineering of human pluripotent cells using TALE nucleases. *Nat. Biotechnol.* **29**, 731–734.

Huang, P., Xiao, A., Zhou, M., Zhu, Z., Lin, S. & Zhang, B. (2011) Heritable gene targeting in zebrafish using customized TALENs. *Nat. Biotechnol.* **29**, 699–700.

Kawai, N., Ochiai, H., Sakuma, T., Yamada, L., Sawada, H., Yamamoto, T. & Sasakura, Y. (2012) Efficient targeted mutagenesis of the chordate Ciona intestinalis genome with zinc-finger nucleases. *Dev. Growth Differ.* **54**, 535–545.

Lawson, N.D. & Weinstein, B.M. (2002) In vivo imaging of embryonic vascular development using transgenic zebrafish. *Dev. Biol.* **248**, 307–318.

Li, L., Piatek, M.J., Atef, A., Piatek, A., Wibowo, A., Fang, X., Sabir, J.S., Zhu, J.K. & Mahfouz, M.M. (2012) Rapid and highly efficient construction of TALE-based transcriptional regulators and nucleases for genome modification. *Plant Mol. Biol.* **78**, 407–416.

Li, T., Huang, S., Zhao, X., Wright, D.A., Carpenter, S., Spalding, M.H., Weeks, D.P. & Yang, B. (2011) Modularly assembled designer TAL effector nucleases for targeted gene knockout and gene replacement in eukaryotes. *Nucleic Acids Res.* **39**, 6315–6325.

Liu, J., Li, C., Yu, Z., Huang, P., Wu, H., Wei, C., Zhu, N., Shen, Y., Chen, Y., Zhang, B., Deng, W.M. & Jiao, R. (2012) Efficient and specific modifications of the Drosophila genome by means of an easy TALEN strategy. *J. Genet. Genomics* **39**, 209–215.

Mahfouz, M.M., Li, L., Shamimuzzaman, M., Wibowo, A., Fang, X. & Zhu, J.K. (2011) De novo-engineered transcription activator-like effector (TALE) hybrid nuclease with novel DNA binding specificity creates double-strand breaks. *Proc. Natl Acad. Sci. USA* **108**, 2623–2628.

McMahon, M.A., Rahdar, M. & Porteus, M. (2012) Gene editing: not just for translation anymore. *Nat. Methods* **9**, 28–31.

Miller, J.C., Tan, S., Qiao, G., *et al.* (2011) A TALE nuclease architecture for efficient genome editing. *Nat. Biotechnol.* **29**, 143–148.

Moore, F.E., Reyon, D., Sander, J.D., Martinez, S.A., Blackburn, J.S., Khayter, C., Ramirez, C.L., Joung, J.K. & Langenau, D.M. (2012) Improved somatic mutagenesis in zebrafish using transcription activator-like effector nucleases (TALENs). *PLoS ONE* **7**, e37877.

Morbitzer, R., Elsaesser, J., Hausner, J. & Lahaye, T. (2011) Assembly of custom TALE-type DNA binding domains by modular cloning. *Nucleic Acids Res.* **39**, 5790–5799.

Morin, X., Daneman, R., Zavortink, M. & Chia, W. (2001) A protein trap strategy to detect GFP-tagged proteins expressed from their endogenous loci in Drosophila. *Proc. Natl Acad. Sci. USA* **98**, 15050–15055.

Mussolino, C. & Cathomen, T. (2012) TALE nucleases: tailored genome engineering made easy. *Curr. Opin. Biotechnol.* **23**, 644–650.

Mussolino, C., Morbitzer, R., Lutge, F., Dannemann, N., Lahaye, T. & Cathomen, T. (2011) A novel TALE nuclease scaffold enables high genome editing activity in combination with low toxicity. *Nucleic Acids Res.* **39**, 9283–9293.

Niwa, H., Yamamura, K. & Miyazaki, J. (1991) Efficient selection for high-expression transfectants with a novel eukaryotic vector. *Gene* **108**, 193–199.

Ochiai, H., Fujita, K., Suzuki, K., Nishikawa, M., Shibata, T., Sakamoto, N. & Yamamoto, T. (2010) Targeted mutagenesis in the sea urchin embryo using zinc-finger nucleases. *Genes Cells* **15**, 875–885.

Ochiai, H., Sakamoto, N., Fujita, K., Nishikawa, M., Suzuki, K., Matsuura, S., Miyamoto, T., Sakuma, T., Shibata, T. & Yamamoto, T. (2012) Zinc-finger nuclease-mediated targeted insertion of reporter genes for quantitative imaging of gene expression in sea urchin embryos. *Proc. Natl Acad. Sci. USA* **109**, 10915–10920.

Reyon, D., Tsai, S.Q., Khayter, C., Foden, J.A., Sander, J.D. & Joung, J.K. (2012) FLASH assembly of TALENs for high-throughput genome editing. *Nat. Biotechnol.* **30**, 460–465.

Sander, J.D., Cade, L., Khayter, C., Reyon, D., Peterson, R. T., Joung, J.K. & Yeh, J.R. (2011) Targeted gene disruption in somatic zebrafish cells using engineered TALENs. *Nat. Biotechnol.* **29**, 697–698.

Sanjana, N.E., Cong, L., Zhou, Y., Cunniff, M.M., Feng, G. & Zhang, F. (2012) A transcription activator-like effector toolbox for genome engineering. *Nat. Protoc.* **7**, 171–192.

Song, X., Sato, Y., Felemban, A., Ito, A., Hossain, M., Ochiai, H., Yamamoto, T., Sekiguchi, K., Tanaka, H. & Ohta, K. (2012) Equarin is involved as an FGF signaling modulator in chick lens differentiation. *Dev. Biol.* **368**, 109–117.

de Souza, N. (2012) Primer: genome editing with engineered nucleases. *Nat. Methods* **9**, 27.

Streubel, J., Blucher, C., Landgraf, A. & Boch, J. (2012) TAL effector RVD specificities and efficiencies. *Nat. Biotechnol.* **30**, 593–595.

Sun, N., Liang, J., Abil, Z. & Zhao, H. (2012) Optimized TAL effector nucleases (TALENs) for use in treatment of sickle cell disease. *Mol. BioSyst.* **8**, 1255–1263.

Takahashi, K., Tanabe, K., Ohnuki, M., Narita, M., Ichisaka, T., Tomoda, K. & Yamanaka, S. (2007) Induction of pluripotent stem cells from adult human fibroblasts by defined factors. *Cell* **131**, 861–872.

Tesson, L., Usal, C., Menoret, S., Leung, E., Niles, B.J., Remy, S., Santiago, Y., Vincent, A.I., Meng, X., Zhang, L., Gregory, P.D., Anegon, I. & Cost, G.J. (2011) Knockout rats generated by embryo microinjection of TALENs. *Nat. Biotechnol.* **29**, 695–696.

Thomas, K.R. & Capecchi, M.R. (1987) Site-directed mutagenesis by gene targeting in mouse embryo-derived stem cells. *Cell* **51**, 503–512.

Tomoda, K., Takahashi, K., Leung, K., Okada, A., Narita, M., Yamada, N.A., Eilertson, K.E., Tsang, P., Baba, S., White, M.P., Sami, S., Srivastava, D., Conklin, B.R., Panning, B. & Yamanaka, S. (2012) Derivation conditions impact X-inactivation status in female human induced pluripotent stem cells. *Cell Stem Cell* **11**, 91–99.

Urnov, F.D., Rebar, E.J., Holmes, M.C., Zhang, H.S. & Gregory, P.D. (2010) Genome editing with engineered zinc finger nucleases. *Nat. Rev. Genet.* **11**, 636–646.

Watanabe, T., Ochiai, H., Sakuma, T., Horch, H.W., Hamaguchi, N., Nakamura, T., Bando, T., Ohuchi, H., Yamamoto, T., Noji, S. & Mito, T. (2012) Non-transgenic genome modifications in a hemimetabolous insect using zinc-finger and TAL effector nucleases. *Nat. Commun.* **3**, 1017.

Weber, E., Gruetzner, R., Werner, S., Engler, C. & Marillonnet, S. (2011) Assembly of designer TAL effectors by Golden Gate cloning. *PLoS ONE* **6**, e19722.

Wood, A.J., Lo, T.W., Zeitler, B., Pickle, C.S., Ralston, E.J., Lee, A.H., Amora, R., Miller, J.C., Leung, E., Meng, X., Zhang, L., Rebar, E.J., Gregory, P.D., Urnov, F.D. & Meyer, B.J. (2011) Targeted genome editing across species using ZFNs and TALENs. *Science* **333**, 307.

Zhang, F., Cong, L., Lodato, S., Kosuri, S., Church, G.M. & Arlotta, P. (2011) Efficient construction of sequence-specific TAL effectors for modulating mammalian transcription. *Nat. Biotechnol.* **29**, 149–153.

Received: 5 November 2012
Accepted: 19 December 2012

Supporting Information

Additional Supporting Information may be found in the online version of this article at the publisher's web site:

Figure S1 hiPSC *HPRT1* knockout mutation analysis.

Figure S2 Bright field and fluorescence microscopy images of *eGFP*_B TALEN-injected frog embryos harboring paternally-transmitted *eGFP* gene.

Figure S3 Sequences observed in *X. laevis* embryos injected with left and right *eGFP*_B TALEN mRNAs. PCR products used for the Cel-I assay (Fig. 6F) were cloned and sequenced.

Table S1 Summary of inverse PCR performed in this study

Table S2 Oligonucleotides for the construction of SSA reporter plasmids

Table S3 Primers for Cel-I assay

Original Contribution : MEMBRANE, 38 (5), 246-253 (2013)

Introduction of a Single Transporter Gene *ABCA3* Directs RLE–6TN to More Type II–like Alveolar Epithelial Cells

Mikihisa Takano[1)]*, Chieko Yamamoto[1)], Keisuke Sambuichi[1)], Keisuke Oda[1)], Junya Nagai[1)], Akira Shimamoto[2)], Hidetoshi Tahara[2)], and Ryoko Yumoto[1)]

1) Department of Pharmaceutics and Therapeutics, Graduate School of Biomedical & Health Sciences, Hiroshima University
1-2-3, Kasumi, Minami–ku, Hiroshima 734-8553, Japan
2) Department of Cellular and Molecular Biology, Graduate School of Biomedical & Health Sciences, Hiroshima University
1-2-3, Kasumi, Minami–ku, Hiroshima 734-8553, Japan

RLE–6TN is a cell line having similar characteristics with those in alveolar type II epithelial cells. However, the development of lamellar bodies, characteristic intracellular structures in type II cells, in RLE–6TN cells is not enough. In this study, RLE–6TN cells were transfected with rat *ABCA3* gene using a retroviral vector, and phenotypical changes were examined. The expression of ABCA3 mRNA and protein as well as the number and size of lamellar body-like structures was increased in RLE/ABCA3 compared with RLE/Vector cells. Surprisingly, not only the expression of ABCA3 mRNA but also the expression of other mRNAs such as SP–A and PEPT2, that are highly expressed in type II cells than in type I cells, was increased in RLE/ABCA3 cells. In contrast, the expression of mRNAs that are highly expressed in type I cells was hardly increased by ABCA3 transfection. In addition, albumin uptake activity, that is much higher in type II cells than in type I cells, was also enhanced in RLE/ABCA3 cells. These results suggest that the introduction of a single transporter gene *ABCA3* would direct RLE–6TN to more type II–like cells, and RLE/ABCA3 cells may be useful as a novel in–vitro model of alveolar type II epithelial cells.

Key words : alveolar epithelial cells / type II cells / ABCA3 / lamellar body / albumin uptake

1. Introduction

In humans, ATP–binding cassette (ABC) transporters and the solute carrier (SLC) transporters are two major superfamilies of membrane transporter proteins. These transporters translocate various nutrients as well as xenobiotics across biomembrane. The ABC transporters are encoded by a large transporter gene family. At present, 49 ABC transporter genes are known to exist in human genome, that are categorized into 7 subfamilies (ABCA to ABCG) based on sequence homology [1~3]. One important function of some ABC transporters is to pump out various toxic xenobiotics from the cells, in order to protect the cells and body. P–Glycoprotein encoded by *ABCB1* (*MDR1*) gene is the most well–known ABC transporter having such function. It is expressed in cancer cells as well as in normal tissues such as the small intestine and the kidney. In the intestine, P–glycoprotein blocks the entry of toxic compounds and drugs across the intestinal epithelial cells, and serves as a first line absorption barrier [4, 5]. Another important function of some other ABC transporters is cellular lipid transport and homeostasis [2]. ABCB4 was recognized first as a phosphatidylcholine transporter, and its activity was found to be closely related to normal liver function [6].

ABCA3 is one of lipid-transporting ABC transporters, and is predominantly expressed in the lung [7]. In the lung, ABCA3 is expressed only in alveolar type II

* Corresponding Author
Tel: +81-82-257-5315
Fax: +81-82-257-5319
E-mail: takanom@hiroshima-u.ac.jp

epithelial cells, and is localized to the limiting membrane of the lamellar bodies [8]. Lamellar body is intracellular organelle for the production, storage, and secretion of pulmonary surfactant from type II cells into alveolar lining fluids. ABCA3 transports surfactant phospholipids into lamellar bodies and therefore the absence of ABCA3 function disrupts lamellar body biogenesis [9]. Now, it is recognized that deficiency of ABCA3 function by genetic mutation leads to lung diseases with fatal pulmonary surfactant deficiency and chronic interstitial lung disease [9].

We have been studying protein and peptide transport function of alveolar epithelial cells, using primary cultured type II cells and transdifferentiated type I-like cells as well as established cell lines [10~13]. RLE-6TN is a cell line established from normal rat lung, and has several characteristics similar to the alveolar type II epithelial cells such as the expression of cytokeratin 19 and alkaline phosphatase activity [10,14]. However, based on morphological observations, we have noticed that the development of lamellar bodies in RLE-6TN cells is not enough compared with that in primary cultured type II cells [15].

As described above, ABCA3 is expressed in type II but not in type I epithelial cells in alveoli, and is essential for lamellar body biogenesis and normal lung function. Therefore, in the present study, we attempted to establish RLE-6TN cells stably expressing rat ABCA3 by gene transfection, in order to obtain a better in-vitro model of alveolar type II epithelial cells. Surprisingly, we observed that the introduction of *ABCA3* gene enhanced not only the expression of ABCA3 mRNA, but also the expression of other mRNAs that were highly expressed in type II cells. Our data suggest that the introduction of a single transporter gene *ABCA3* would direct RLE-6TN to more type II-like alveolar epithelial cells.

2. Experimental Section

2.1 Materials

RLE-6TN cells were obtained from the American Type Culture Collection (ATCC no. CRL-2300; Manassas, VA, USA). Fetal bovine serum (FBS), Dulbecco's modified Eagle medium (DMEM), and Nutrient Mixture F-12 (Ham) were purchased from MP Biomedicals (Solon, OH, USA). pGEM T-Easy vector, T4 DNA Ligase, restriction enzymes such as Sph I and Not I were purchased from Promega (Madison, WI, USA). pMXs-Puro Retroviral Vector and GenePORTER 2 were purchased from Cell Biolabs, Inc. (San Diego, CA, USA) and from Genlantis (San Diego, CA, USA), respectively. Plat-E cells, which were used for the production of retroviruses, were kindly provided from Dr. Toshio Kitamura [16]. Trypsin-EDTA, penicillin-streptomycin, and LysoTracker® Red DND-99 (LysoTracker Red) as a fluorescent marker for lamellar bodies were purchased from Life Technologies (Carlsbad, CA, USA). Nile red as a selective fluorescent stain for intracellular lipid droplets in lamellar bodies was purchased from COSMO BIO Co. Ltd. (Tokyo, Japan). Hoechst 33342 solution as a fluorescent nucleus marker was purchased from Wako Pure Chemical Ind. (Osaka, Japan). Antibodies against ABCA3 (P180 Lamellar Body Protein Antibody [3C9] (ab24751)) and secondary antibodies (Goat polyclonal Secondary Antibody to Mouse IgG-H&L (FITC) (ab6785)) were purchased from Abcam plc. (Cambridge, UK). Bovine serum albumin fraction V, fluorescein isothiocyanate-labeled bovine serum albumin (FITC-albumin), and puromycin were purchased from Sigma-Aldrich (St. Louis, MO, USA). ReverTra Ace®, ReverTra Dash®, and THUNDERBIRD® SYBER® qPCR Mix were from TOYOBO (Osaka, Japan). Vectashield mounting medium (H-1000) was from Vector laboratories, Inc. (Burlingame, CA, USA). All other chemicals used for the experiments were of the highest purity commercially available.

2.2 Vector construction

Full-length rat *ABCA3* gene (accession No. XM-001054650) was constructed from two separated fragments, A and B. The primers used for the amplification of these fragments were: ABCA3-fragment A-F383 (5'-AGCAACCTTTCCTGGAACTAAGTTGT-3'), ABCA3-fragment A-R2365 (5'-TTCAGGACACTTCTGGACAGAGAGG-3'), ABCA3-fragment B-F2199 (5'-CAGGTCTCTTCCCCCCTACCAGTG-3'), ABCA3-fragment B-R5687 (5'-ATATCACCTTGATTCTTGTCATGTCC-3'). Each fragment was amplified by RT-PCR using ReverTra Dash. The PCR conditions were as follows: initial denaturation in one cycle of 5 min at 95 ℃, 35 cycles with 30 s at 95 ℃ (denaturation), 30 s at 60 ℃ (annealing), and 1.5 min (fragment A) or 3 min (fragment B) at 72 ℃ (exten-

Table 1 Primer sequences for real-time PCR

Gene Name	Accession Number	Sequence (F: forward R: reverse)	Position of Amplified DNA (bp)	Product Size (bp)
Type II Marker				
ABCA3	XM_001054650	F 5'-TTTCGTGGCTCCTCGGTACAACTG-3'	1622-1645	215
		R 5'-GTACTGAATCCAGCAGCAGCATCC-3'	1813-1836	
SP-A	NM_001270647	F 5'-TGAAGTCAGAGGCATCCA-3'	43-60	180
		R 5'-ACCTGTCACATTAGCATAGC-3'	203-222	
SP-B	NM_138842	F 5'-GTGCCTTTCTGCAAGTCTGA-3'	723-747	75
		R 5'-ACCAGGCCACAGACTAGCT-3'	777-797	
SP-C	NM_017342	F 5'-CTGAGATGGTCCTTGAGAT-3'	205-223	108
		R 5'-CAGTGGAGCCAATAGAGA-3'	295-312	
PEPT2	NM_031672	F 5'-GCATGAAAGCTGTGCTGACCTTGT-3'	357-380	191
		R 5'-ATGGCCAAGAACATACACCAGGGA-3'	524-547	
MRP2	NM_012833	F 5'-TGATCGGTTTCGTGAAGAGC -3'	1119-1138	139
		R 5'-ACGCACATTCCCAACACAAA-3'	1238-1257	
Type I Marker				
IGFBP6	NM_013104	F 5'-CCGCAGACACTTGGATTCAGT-3'	446-466	62
		R 5'-TTGCTCCGCCTCTGAAGAC-3'	489-507	
BCRP	NM_181381	F 5'-ATGATGCTCTTTTCTGGCCTCT-3'	1723-1744	92
		R 5'-AAGCCATATCGAGGAATGCTAAA-3'	1792-1814	
Caveolin-1	NM_031556	F 5'-CAGCATGTCTGGGGGTAAAT-3'	36-55	123
		R 5'-TGCTTCTCATTCACCTCGTCT-3'	138-158	
SGLT2	NM_022590	F 5'-AAAATACGGCAGGAAGGAACTG-3'	2117-2138	97
		R 5'-GACAAATTGGCCACCATCTTG-3'	2193-2213	
GAPDH	NM_017008	F 5'-AGCCCAGAACATCATCCCTG-3'	675-694	161
		R 5'-CACCACCTTCTTGATGTCATC-3'	855-835	

ABCA3: ATP-binding cassette, sub-family A (ABCA), member 3; SP-A, B, C: Surfactant protein A, B, C; PEPT2: Peptide transporter 2; MRP2: Multidrug resistance-associated protein 2; IGFBP6: Insulin-like growth factor-binding protein 6; BCRP (ABCG2): Breast cancer resistance protein; SGLT2: Sodium-dependent glucose transporter 2; GAPDH: Glyceraldehyde-3-phosphate dehydrogenase (a house keeping gene)

sion). The reaction was completed at an elongation temperature of 72 ℃ for 5 min. The PCR product of fragment A or B was purified and each fragment was cloned into pGEM T-Easy vector. Each plasmid was digested by Sph I, and isolated fragment B was ligated into fragment A-containing vector by T4 DNA Ligase, in order to construct pGEM T-Easy vector containing full-length rat *ABCA3* gene. Finally, the plasmid was digested by Not I and *ABCA3* gene isolated was cloned into Not I site of pMXs-Puro Retroviral Vector.

2.3 Retrovirus infection

Retroviruses were generated by transfecting retroviral vector (ABCA3 or empty vectors) into Plat-E cells using GenePORTER 2. Supernatants were collected at 48 hr after transfection, filtered through a membrane (pore size; 0.45 μm), and directly used to infect RLE-6TN cells. Infected cells were subcultured at 48 hr after infection, and were subcultured again after another 48 hr. Then, RLE/ABCA3 and RLE/Vector cells stably expressing transfected gene were selected with the culture medium containing 1.6 μg/ml puromycin.

2.4 The expression level of various mRNAs in RLE/ABCA3 and RLE/Vector cells

Cells were cultured for 7 days on 35-mm culture dishes. Total RNA was extracted from the cells with an RNeasy Mini Kit (Qiagen, Hilden, Germany). The total RNA was reverse transcribed into cDNA by using Rever Tra Ace.

Real-time PCR was performed on CFX Connect Realtime-PCR system (Bio-Rad Laboratories, Hercules, CA, USA) using THUNDERBIRD SYBR qPCR Mix. The reaction mixtures consisted of 2 μl cDNA which was diluted 4 times with DEPC treated water, 5 μl THUNDERBIRD SYBR qPCR Mix, and primers, in a final volume of 10 μl. The PCR conditions were: initial denaturation for one cycle of 1 min at 95 ℃, followed by specified cycles of 10 s at 95 ℃ (denaturation), 15 s at 60 ℃ (annealing), and 15 s at 72 ℃ (extension). After the reaction, a melting curve was obtained to confirm the single product. The primers used in the present study were shown in Table 1. The expression level of mRNA was normalized as to that of glyceraldehyde-3-phosphate dehydrogenase (GAPDH), a housekeeping gene.

2.5 Cell culture

Cells were cultured in DMEM/F-12 (1 : 1) containing 10% FBS, 100 IU/ml penicillin, and 100 mg/ml streptomycin, in an atmosphere of 5% CO_2-95% air at 37 ℃, and subcultured every 7 days using 0.25% trypsin and 1 mM EDTA as described previously [10, 17]. Fresh

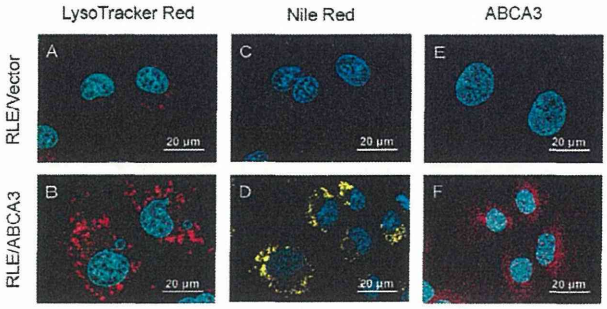

Fig. 1 Confocal laser scanning micrographs of RLE/Vector (A, C, E) and RLE/ABCA3 (B, D, F) cells (passage #35). A, B: LysoTracker red (red) and C, D: Nile red (yellow) for lamellar body staining; E, F: Immunostaining of ABCA3 (red), and Hoechst 33342 (blue) for nuclear staining.

medium was replaced every 2 days, and the cells (passages; 20 to 35) were used for the experiments on the seventh day after seeding.

2.6 Confocal laser scanning microscopy

The cells grown on 35–mm glass bottom culture dishes for 4 days were incubated at 37 ℃ with LysoTracker Red (75 nM) and Hoechst 33342 (10 μM) for 30 min, or with Nile red (1 μM) for 60 min. Then, the cells were washed with ice–cold phosphate–buffered saline (PBS buffer; 137 mM NaCl, 3 mM KCl, 8 mM Na_2HPO_4, 1.5 mM KH_2PO_4, 0.1 mM $CaCl_2$, and 0.5 mM $MgCl_2$, pH 7.4) three times for 5 min each.

For the detection of ABCA3 by immunostaining, cells grown on 35–mm glass bottom culture dishes were fixed with 2% paraformaldehyde in PBS buffer for 30 min, and permeabilized with 0.25% Triton X–100 for 10 min and blocked for 60 min in PBS buffer containing 1% bovine serum albumin fraction V at room temperature. The cells were washed two times with PBS buffer between each step. The cells were incubated with primary antibodies against ABCA3 (1 : 500 dilution) for 2 hr at room temperature. After washing three time with PBS buffer, the cells were incubated with FITC–labeled secondary antibodies (1 : 1000 dilution) for 1 hr and then with 10 μM Hoechst 33342 (for nuclear staining) for 30 min at room temperature. Finally, the cells were treated with Vectashield mounting medium.

Each fluorescence in the cells was visualized by confocal laser scanning microscopy (LSM5 Pascal, Carl ZEISS Microimaging GmbH, Jena, Germany) using a 63X oil immersion objective lens.

2.7 Uptake studies

Uptake experiments were performed as described previously [10, 13, 17]. Cells grown on 12–well culture plates were used. After removal of the culture medium, each well was washed and preincubated with 1 ml of PBS buffer supplemented with 5 mM D–glucose (PBS–G buffer) at 37 ℃ for 10 min. Then, 0.5 ml of PBS–G buffer containing FITC–albumin (20 μg/ml or 20 mg/ml) was added to each well, and the cells were incubated at 37 ℃ for a specified period.

At the end of the incubation, the uptake buffer was aspirated and the cells were washed rapidly three times with 1 ml of ice–cold PBS buffer. The cells were scraped with a rubber policeman into 0.75 ml of ice-cold PBS buffer and the wells were rinsed again with 0.75 ml of ice–cold PBS buffer to improve the recovery of the cells. The cells were further washed by centrifugation at 4 ℃ for 3 min at 9,838 g twice. After the supernatant was aspirated, the pellet was solubilized in 1 ml of 0.1% Triton X–100 in PBS buffer without $CaCl_2$ and $MgCl_2$ at room temperature for 30 min, and centrifuged for 3 min at 5,600 g. The supernatant was used for fluorescence and protein assays. The amount of FITC–albumin taken up by the cells was measured using a Hitachi fluorescence spectrophotometer F–2700 (Tokyo, Japan) at an excitation wavelength of 500 nm and an emission wavelength of 520 nm. Protein was determined by the Lowry method with bovine serum albumin as the standard.

2.8 Statistical analysis

Data were expressed as means ± S.E.. Statistical analysis was performed by Student's *t*–test. The level of significance was set at $*p < 0.05$ or $**p < 0.01$.

3. Results and Discussion

3.1 Formation of lamellar body–like structures in RLE/ABCA3 cells

The alveolar region of the lung is lined with a continuous epithelium comprising two major types of epithelial cells, type I and type II [18]. Alveolar type I epithelial cells have a squamous morphology, and are essential for gas exchange. On the other hand, type II cells are cuboidal epithelial cells, and have a characteristic intracellular structure called lamellar body, which would play important roles for surfactant production and

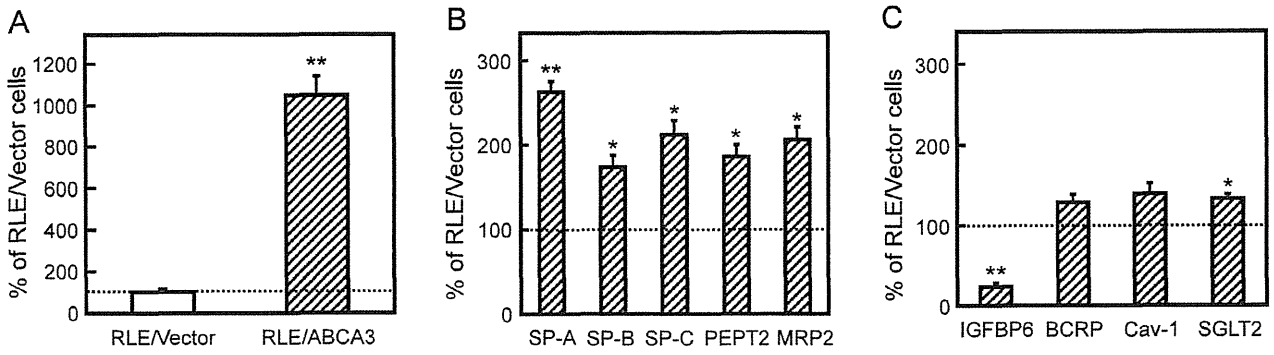

Fig. 2 The expression of mRNAs of ABCA3 (A), Type II marker (B), and Type I marker (C) in RLE/Vector and RLE/ABCA3 cells (passage #34). Total RNA was extracted from RLE/Vector and RLE/ABCA3 cells, and real-time PCR analysis was performed to evaluate the expression of each mRNA. The percentage of RLE/Vector cells of each mRNA expression in RLE/ABCA3 cells was calculated after normalization by the expression of GAPDH, a housekeeping gene. Cav-1: caveolin-1. Each value represents the mean ± S.E. of three RNA samples. $*p < 0.05$ and $**p < 0.01$; significantly different from the value in RLE/Vector cells.

secretion. Therefore, we first examined and compared the formation of lamellar body-like structures in RLE/Vector cells and in RLE/ABCA3 cells, which were stable transfectants established by the transfection with a retroviral vector (mock-transfected) and a retroviral vector containing *ABCA3* gene, respectively. In order to observe intracellular lamellar body-like structures by the confocal laser scanning microscopy, these cells were stained with LysoTracker Red (an acidic organelle-selective cell-permeant fluorescence probe) and with Nile red (fluorescence probe for the staining of intracellular lipid droplets), as described previously [15, 19]. As shown in Fig. 1A-D, lamellar body-like structures stained with LysoTracker Red and Nile red were more evident in RLE/ABCA3 cells compared with those in RLE/Vector cells. We have previously showed the confocal laser scanning micrographs of primary cultured rat alveolar type II cells, in which lamellar bodies were clearly stained with LysoTracker Red and Nile red [15]. Lamellar body-like structures observed in RLE/ABCA3 cells in this study were quite similar with those observed in type II cells. On one hand, A549 is an epithelial cell line derived from human lung carcinoma, and has been widely used as an in vitro model of human alveolar type II epithelial cells for biochemical and toxicological studies [13]. However, like RLE-6TN cells, the development of lamellar bodies in A549 cells is also poor (data not shown). In this context, RLE/ABCA3 cells may be a better in-vitro model of alveolar type II epithelial cells than RLE-6TN cells and/or A549 cells.

Nagata et al. also reported that the formation of lamellar body-like structures could be observed after *ABCA3* gene transfection, though the cells they used were HEK293 cells derived from human embryonic kidney and not alveolar epithelial cells [20]. Cheong et al. examined the effects of *ABCA3* gene disruption in mice [21]. They found that homozygous ABCA3 $^{-/-}$ knock-out mice died soon after birth, and alveolar type II cells from ABCA3 $^{-/-}$ embryos contained no lamellar bodies. Thus, ABCA3 is critical for lamellar body biogenesis, and increased formation of lamellar body-like structures observed in RLE/ABCA3 cells would be due to the enhanced expression of ABCA3. The enhanced expression of ABCA3 protein in RLE/ABCA3 cells was confirmed by immunostaining using antibody for ABCA3 (Fig. 1E, F).

3.2 Expression of ABCA3 and other mRNAs in RLE/ABCA3 cells

The expression of ABCA3 mRNA was estimated in RLE/ABCA3 cells. As expected, the expression level of ABCA3 mRNA in RLE/ABCA3 cells was about 10-fold higher than in RLE/Vector cells (Fig. 2A). The expression of other mRNAs was also examined. At first, we carried out these experiments to confirm that only ABCA3 but no other mRNA expression would be changed. Surprisingly, however, the expression of some other mRNAs such as SP-A, SP-B, SP-C, PEPT2, and MRP2 was also increased (Fig. 2B). SP-A, SP-B and SP-C are surfactant proteins which regulate the structural and functional integrity of pulmonary

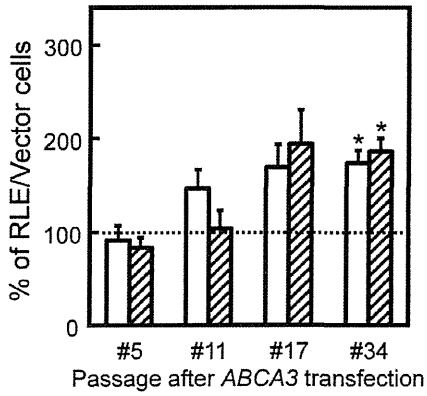

Fig. 3 Effect of passage after *ABCA3* transfection on the expression of SP–B (open columns) and PEPT2 (hatched columns) in RLE/ABCA3 cells. The percentage of RLE/Vector cells of each mRNA expression in RLE/ABCA3 cells was calculated after normalization by the expression of GAPDH, a housekeeping gene. Each value represents the mean ± S.E. of three RNA samples. * $p<0.05$; significantly different from the value in RLE/Vector cells.

surfactant [22]. SP–A, together with SP–B, is required for conversion of secreted endogenous surfactant to tubular myelin in the alveolar lining. SP–B may selectively remove anionic and unsaturated lipid species from the alveolar surface film, thereby increasing surface pressure. SP–C accelerates the adsorption of lipid bilayers to an interfacial monolayer [22]. PEPT2 (SLC15A2) is a peptide transporter, and transports various di– and tri– peptides through secondary active transport coupled with an electrochemical proton gradient [23]. MRP2 (ABCC2) is an ATP–dependent efflux transporter (pump), and transports various organic anions through primary active transport [4]. The mRNAs of these proteins are highly expressed in alveolar type II epithelial cells compared with type I cells, and therefore assumed to be type II cell marker mRNAs [11, 24]. On the other hand, the expression of mRNAs highly expressed in type I cells compared with type II cells (type I cell marker mRNAs) such as IGFBP6, BCRP, and Caveolin–1 was not significantly increased by *ABCA3* gene transfection, though the expression of SGLT2 was significantly but only slightly increased (Fig. 2C).

In the lung, type II cells are known to serve as progenitor cells of type I cells, and transdifferentiate into type I cells to repair the epithelium when it is injured [25]. Such a transdifferentiation of type II cells into type I cells (also referred as type I–like cells) also occurs under in–vitro conditions. We have previously examined the transdifferentiation of primary cultured rat alveolar type II cells into type I cells [11]. We found that the morphology of the cells were markedly changed between type II and type I cells, and lamellar bodies were almost completely disappeared in type I cells. In addition, the expression of type II cell marker mRNAs such as SP–B and chemokine-induced neutrophilic chemoattractant–1 was drastically decreased along with the transdifferentiation. Therefore, the enhanced expression of some type II cell marker mRNAs may indicate that type II phenotype was potentiated by introducing *ABCA3* gene into RLE–6TN cells.

3.3 Expression of type II marker mRNAs along with passages of RLE/ABCA3 cells

The expression of SP–B and PEPT2, type II cell marker mRNAs, was evaluated in RLE/ABCA3 cells with different passages. As shown in Fig. 3, the expression of these mRNAs became higher along with the passages of the cells. These results indicate that the number of cell passages and/or time after gene transfection may be an important factor for the regulation of the expression of other mRNAs than ABCA3.

As described above, Cheong et al. examined the role ABCA3 using *ABCA3* $^{-/-}$ knock–out mice, and concluded that ABCA3 is necessary for lamellar body biogenesis [21]. In the study, they observed that the expression of mature SP–B protein was disrupted, while pro–SP–B precursor level was not changed in alveolar type II cells from *ABCA3* $^{-/-}$ embryos, indicating that *ABCA3* $^{-/-}$ knock–out would affect SP–B processing rather than its expression. On the other hand, in this study, enhanced expression of SP–B mRNA was observed in ABCA3–overexpressing RLE/ABCA3 cells. Though the animal species (mouse vs. rat) and experimental settings (in vivo vs. in vitro) are different, the reason for this apparent inconsistency concerning the relationship between ABCA3 and SP–B expression is not clear at this moment and needs to be studied further.

3.4 Effect of ABCA3 gene introduction on albumin uptake activity

We have been studying the uptake of albumin in primary cultured alveolar epithelial cells as well as established cell lines such as RLE–6TN and A549 [10, 11, 13, 17].

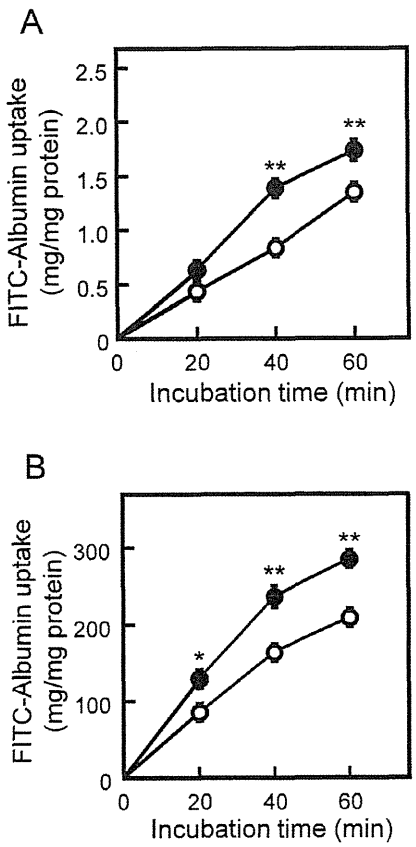

Fig. 4 High (A)- and low (B)- affinity transport of FITC-albumin in RLE/ABCA3 (closed circles) and RLE/Vector (open circles) cells. (A) Uptake of FITC-albumin (20 μg/ml) by confluent monolayers of the cells (passage #20) was measured at 37 ℃. (B) Uptake of FITC-albumin (20 mg/ml) by confluent monolayers of the cells (passage #25) was measured at 37 ℃. Each point represents the mean ± S.E. of 3 monolayers. $^{*}p < 0.05$ and $^{**}p < 0.01$; significantly different from the value in RLE/Vector cells.

The uptake of albumin in RLE-6TN cells was mediated by high- and low-affinity transport systems, and clathrin-mediated endocytosis was involved in both transport systems [10, 17]. The Km (Michaelis constant) values for high- and low-affinity albumin transport systems in RLE-6TN cells were 0.13 mg/ml (1.9 μM) and 8.7 mg/ml (130 μM), respectively [10]. In addition, albumin uptake activity (uptake amount/mg cell protein) was about 5-fold higher in type II cells than in type I cells [11]. Therefore, the higher albumin uptake activity is one of characteristic features of type II cells. Based on these backgrounds, we evaluated the albumin uptake activity in RLE/ABCA3 cells and RLE/Vector cells. FITC-albumin was used as a substrate at a concentration of 20 μg/ml for evaluating a high-affinity transport system and 20 mg/ml for evaluating a low-affinity transport system, respectively [10, 17]. As shown in Fig. 4A, the high-affinity uptake of FITC-albumin was time-dependent, and increased up to 60 min in both RLE/ABCA3 cells and RLE/Vector cells. The uptake activity of FITC-albumin was significantly higher in RLE/ABCA3 cells than in RLE/Vector cells. Similar results were observed in the low-affinity uptake of FITC-albumin (Fig. 4B). Thus, in addition to the enhanced expression of type II cell marker mRNAs, enhanced uptake of albumin in RLE/ABCA3 cells would also support the idea that type II phenotype was potentiated by introducing *ABCA3* gene into RLE-6TN cells. The important physiological function of alveolar type II cells is to produce pulmonary surfactant containing various surfactant proteins. As shown in Fig. 1, lamellar bodies were well developed in RLE/ABCA3 cells compared with RLE/Vector cells. Therefore, in RLE/ABCA3 cells, the increased uptake of proteins, peptides, and/or amino acids may be needed to support the de novo synthesis of surfactant proteins in the cells.

Though the molecular mechanism underlying the enhancement of albumin uptake in RLE/ABCA3 cells is not clear, the expression of a putative receptor for albumin endocytosis might be affected by the introduction of *ABCA3* gene into RLE-6TN cells. We have previously discussed the possible receptors involved in clathrin-mediated endocytosis of albumin in RLE-6TN cells, including megalin and cubilin [10]. More recently, Buchäckert et al. [26] reported that megalin would mediate transepithelial albumin clearance from the alveolar space of intact rabbit lungs, indicating that megalin should be a possible receptor for albumin endocytosis in alveolar epithelial cells. However, the role of megalin in alveolar transport of albumin is still controversial, and needs to be explored further. Identification of albumin receptor in alveolar epithelial cells would help to clarify the mechanism of enhanced albumin uptake in RLE/ABCA3 cells.

In order to confirm the effect of *ABCA3* gene introduction on the phenotype of RLE-6TN cells, we also established ABCA3-overexpressing RLE-6TN cells by another transfection method, lipofection, using pIRESpuro2 Vector. Though the transfection efficiency was much lower compared with the retroviral vector, ABCA3-overexpressing RLE-6TN cells (RLE/

ABCA3/Lipo cells) were obtained, and lamellar body structures, mRNA expression, and albumin uptake were examined and compared with those in mock-transfected cells. Similar findings with those in RLE/ABCA3 cells established by the retrovirus infection were observed in RLE/ABCA3/Lipo cells (data not shown).

At present, gene transfection is a common technique employed to study the function of the protein encoded by the gene. However, the present results suggest that much attention should be paid whether or not other functions are affected by the single gene transfection. The mechanism underlying the phenotypical changes induced by *ABCA3* gene transfection is not clear. However, it may be related to the enhanced formation of lamellar body-like structures. As described, lamellar body has important roles in the production, storage, and secretion of pulmonary surfactant from type II cells into alveolar lining fluids [8, 27]. Therefore, increased secretion of surfactant components would occur in RLE/ABCA3 cells, which may affect the phenotype of the cells. Further studies are needed to clarify these points.

In conclusion, introduction of a single transporter gene *ABCA3* would direct RLE-6TN to more type II-like alveolar epithelial cells, as evidenced by enhanced formation of lamellar body-like structures, enhanced expression of type II marker mRNAs, and enhanced albumin uptake activity. RLE/ABCA3 cells may be useful as a novel in-vitro model of alveolar type II epithelial cells.

Acknowledgement

We thank the Analysis Center of Life Science, Hiroshima University, for the use of their facilities. This work was supported in part by a Grant-in-Aid for Scientific Research from Japan Society for the Promotion of Science (JSPS).

References

1) Dean M, Rzhetsky A, Allikmets R : *Genome Res.*, **11**, 1156-1166 (2001)
2) Takahashi K, Kimura Y, Nagata K, Yamamoto A, Matsuo M, Ueda K : *Med. Mol. Morphol.*, **38**, 2-12 (2005)
3) Huang Y : *Cancer Metastasis Rev.*, **26**, 183-201 (2007)
4) Takano M, Yumoto R, Murakami T : *Pharmacol. Ther.*, **109**, 137-161 (2006)
5) Murakami T, Takano M : *Expert Opin. Drug Metab. Toxicol.*, **4**, 923-939 (2008)
6) Smit JJM, Schinkel AH, Elferink RPJO, Groen AK, Wagenaar E, van Deemter L, Mol CAAM, Ottenhoff R, van der Lugt NMT, van Roon MA, van der Valk MA, Offerhaus GJA, Berns AJM, Borst P : *Cell*, **75**, 451-462 (1993)
7) Klugbauer N, Hofmann F : *FEBS Lett.*, **391**, 61-65 (1996)
8) Yamano G, Funahashi H, Kawanami O, Zhao LX, Ban N, Uchida Y, Morohoshi T, Ogawa J, Shioda S, Inagaki N : *FEBS Lett.*, **508**, 221-225 (2001)
9) Weichert N, Kaltenborn E, Hector A, Woischnik M, Schams A, Holzinger A, Kern S, Griese M : *Respir. Res.*, **12**, 4-12 (2011)
10) Yumoto R, Nishikawa H, Okamoto M, Katayama H, Nagai J, Takano M : *Am. J. Physiol. Lung Cell. Mol. Physiol.*, **290**, L946-L955 (2006)
11) Ikehata M, Yumoto R, Nakamura K, Nagai J, Takano M : *Pharm. Res.*, **25**, 913-922 (2008)
12) Oda K, Yumoto R, Nagai J, Katayama H, Takano M : *Eur. J. Pharmacol.*, **672**, 62-69 (2011)
13) Yumoto R, Suzuka S, Oda K, Nagai J, Takano M : *Drug Metab. Pharmacokinet.*, **27**, 336-343 (2012)
14) Driscoll KE, Carter JM, Iype PT, Kumari HL, Crosby LL, Aardema MJ, Isfort RJ, Cody D, Chestnut MH, Burns JL, et al. : *In Vitro Cell. Dev. Biol. Anim.*, **31**, 516-527 (1995)
15) Takano M, Yumoto R : *Membrane*, **36**, 145-153 (2011)
16) Morita S, Kojima T, Kitamura T : *Gene Ther.*, **7**, 1063-1066 (2000)
17) Tagawa M, Yumoto R, Oda K, Nagai J, Takano M : *Drug Metab. Pharmacokinet.*, **23**, 318-327 (2008)
18) Patton JS : *Adv. Drug Deliv. Rev.*, **19**, 3-36 (1996)
19) Takano M, Horiuchi T, Nagai J, Yumoto R : *Lung*, **190**, 651-659 (2012)
20) Nagata K, Yamamoto A, Ban N, Tanaka AR, Matsuo M, Kioka N, Inagaki N, Ueda K : *Biochem. Biophys. Res. Commun.*, **324**, 262-268 (2004)
21) Cheong N, Zhang H, Madesh M, Zhao M, Yu K, Dodia C, Fisher AB, Savani RC, Shuman H : *J. Biol. Chem.*, **282**, 23811-23817 (2007)
22) Johansson J, Curstedt T, Robertson B : *Eur. Respir. J.*, **7**, 372-391 (1994)
23) Terada T, Saito H, Mukai M, Inui K : *Am. J. Physiol.*, **273**, F706-F711 (1997)
24) Gonzalez R, Yang YH, Griffin C, Allen L, Tigue Z, Dobbs L : *Am. J. Physiol. Lung Cell. Mol. Physiol.*, **288**, L179-L189 (2005)
25) Fehrenbach H : *Respir. Res.*, **2**, 33-46 (2001)
26) Buchäckert Y, Rummel S, Vohwinkel CU, Gabrielli NM, Grzesik BA, Mayer K, Herold S, Morty RE, Seeger W, Vadász I : *J. Physiol.*, **590**, 5167-5181 (2012)
27) Ban N, Matsumura Y, Sakai H, Takanezawa Y, Sasaki M, Arai H, Inagaki N : *J. Biol. Chem.*, **282**, 9628-9634 (2007)

(Received 17 July 2013 ;
Accepted 9 August 2013)